Faraday Discussions

Attosecond electronic delay response in dielectric materials

Journal:	*Faraday Discussions*
Manuscript ID	FD-ART-01-2022-000002
Article Type:	Paper
Date Submitted by the Author:	06-Jan-2022
Complete List of Authors:	Alqattan, Husain; The University of Arizona, Physics Hui, Dandan; The University of Arizona, Physics Sennary, Mohamed ; The University of Arizona, Physics Hassan, Mohammed; The University of Arizona, Physics

TITLE

Attosecond electronic delay response in dielectric materials

AUTHORS

Husain Alqattan†, Dandan Hui †, Mohamed Sennary and Mohammed Th. Hassan*

AFFILIATIONS

Department of Physics, University of Arizona, Tucson, AZ 85721, USA.

***Author to whom correspondence should be addressed:** mohammedhassan@email.arizona.edu

†These authors contributed equally to this work.

Abstract

The advancement in the attosecond field and the generation of XUV attosecond pulses enabled the study of electron dynamics in solid-state by high harmonic generation spectroscopy. Here, we introduce new all-optical attosecond metrology to study the light-field induced electron dynamics in dielectric systems. This new methodology is based on the phase transition of dielectric due to interaction with strong light field. Hence, the charge carriers undergo an inter- and intraband band transition, causing a modification in the electronic structure, dielectric constant, and optical properties of the dielectric system. Consequently, the dielectric experiences an adiabatic semi-metal phase transition due to the strong polarizability. Therefore, the reflectivity of the dielectric systems is changing following the shape of the pump field. Accordingly, the time-resolved reflectivity change measurement provides direct access to the phase transition and the related electronic dynamics of the system in real-time.

In the reported experiment, a strong light field (pump pulse) induces the phase transition and modifies the fused silica sample reflectivity, which is probed by another weak light field (probe pulse). The reflected probe beam spectrum is acquired as a function of the time delay between the pump and probe pulses. This measurement shows that the real-time phase transition dynamic (and reflectivity change) follows the pump field shape. Moreover, the reflectivity measurements have been recorded at different pump field strengths performed under the same conditions. The reflectivity trace shows a retardation phase delay at higher driver field strength. The delay response —retrieved from the recorded reflectivity traces— is on the order of a few hundred attoseconds. In addition, the results show that the delay response monotonically increases as the trigger field escalates. Furthermore, the reflectivity measurements have been acquired for another dielectric system (CaF_2). The electronic delay response shows the same linear behavior increase as SiO_2 system. This work establishes universal new attosecond metrology for measuring the electron dynamics and delay response in different materials.

Introduction

Earlier, it was thought that chemical processes were immeasurably fast. Although, using the ultrashort laser pulses in femtosecond time-resolved spectroscopy measurements provided access to the structural dynamics in chemical reactions[1]. This revolutionary advance provided information about the transition states in real-time and gave birth to the ultrafast science and femtochemistry fields[2]. Later, different ultrafast laser spectroscopic techniques were developed to trace the atomic motion of matter. Although, capturing the electronic motion on a femtosecond or less timescale remained beyond reach due to the temporal resolution limit.

Studying the electron dynamics on its native time scale is the key to understanding and controlling the quantum mechanical underpinnings of physical and chemical dynamics of matter[3-5]. In the last two decades, the generation of attosecond extreme ultraviolet (XUV) pulses spectroscopy[6-12]—based on a high harmonic generation process—has permitted the real-time observation of electron motion dynamics in atoms, molecules, and the solid-state[4, 5, 10-15]. Although, the development of attosecond XUV spectroscopy allowed us to explore the electronic response of atoms and solids in the ionized state only. Recently, the development of the synthesized attosecond laser pulses[16] enabled the determination of the nonlinear response of bound electrons dynamics in the atomic system, which was determined to be in the order of a hundred attoseconds[16-18]. Although, the electronic delay response of bound electrons in solid states is not reported yet.

Here, we study the excited carrier dynamics and the related phase transition in dielectric systems to determine the relative electronic delay response in the presence of a strong light field. Previously, the underlying physics of strong-field interaction with dielectric solid-state systems and the associated electron and optical reflectivity dynamics were probed by XUV spectroscopy using a high-energy photon. Although, it was demonstrated that the tracing of the optical reflectivity modulation would provide direct insights to the electronic response and the phase transition dynamics of the dielectric material[19]. The strong field-induced electron dynamics in dielectric have been studied intensively theoretically and experimentally[6-9, 19-25]. Based on these studies, the charge carriers are first excited from the valance band to the conduction band via multiphoton excitation through virtual state[21]. Then, the excited electrons in the conduction band move in the reciprocal space by acquiring a time-dependent momentum from the driving field[19-

[23, 25, 26]. Thus, the electrons are accelerated and decelerated following the shape of the pump field's vector potential, altering the electronic structure and the optical properties of the system[19-28].

In this work, we study the electronic delay response and its relation to the intensity of the external triggering field in different dielectric systems. Our study exploited the attosecond all-optical reflectivity modulation (Atto-ARM) methodology[19] to measure the reflectivity modulation of the SiO_2 (band gap= 9eV) dielectric system triggered by the strong field interaction of the few-cycle visible laser pulses. From these measurements, we obtain the total reflectivity modulation (TRM) trace of the SiO_2 as a function of the time delay between the pump and probe pulses, which carries the signature of the transient phase-transition dynamics of the dielectric following the vector potential of the pump field. Moreover, we measured the TRM traces at different field intensities and determined the relative phase delay retardation between these traces due to the electronic delay response of the SiO_2. Furthermore, we determined the relative electronic delay response of calcium fluoride (CaF_2), which has a higher bandgap (12eV), using the same methodology. Finally, the presented measurements allowed us to compare the electronic dynamics behaviors in the two different dielectric materials.

Method

Experimental setup

In this work, we conducted two experiments using the Atto-ARM[19] setup arrangement illustrated in Fig. 1a to study the transient phase transition dynamics, the reflectivity modulation in real-time, and the electronic response of two dielectric systems; SiO_2 and CaF_2. The experiment setup can be described as follows: high-power (1mJ) multi-cycle pulses are generated from optical parametric chirped-pulse amplification (OPCPA) laser system. These multi-cycle pulses are nonlinearly propagated inside a Hollow-Core Fiber (HCF) filled with pressurized Neon gas (2 bar). A powerful broadband spectrum that spans the visible and near-infrared spectral regions is generated. A chirped mirror compressor is used to compress the spectrum region from 500-700 nm (see Fig. 1b) to its Fourier-limit duration (6.5 fs). The Carrier-Envelope-Phase (CEP) of these pulses is passively locked with an estimated phase jittering of ~100 mrad. Then, the output linearly polarized (p-pol) beam from the compressor is divided by a two-hole mask into two beams. The first beam that emerges from the first hole (diameter = 3 mm) has a high intensity (pump beam). In contrast, the

second beam (probe beam) has lower intensity since it is emerging from a smaller diameter hole (1 mm). The second beam intensity is about ~3.3% of the first beam intensity. The two beams are co-linearly propagated to two identical D-shape focusing mirrors (f =100mm) and then focused by a small incident angle on a 100 μm SiO_2 sample. One of the two D-shape mirrors is carried on a high-precise piezo positing stage. This stage controls the arriving time (on the sample) and the delay between the two beams with attosecond resolution. The input beam intensity is controlled by a round continuously variable metallic neutral density filter introduced in the beam path (see Fig. 1a), by changing the rotatory angle of the filter so the propagation length inside the filter is constant.

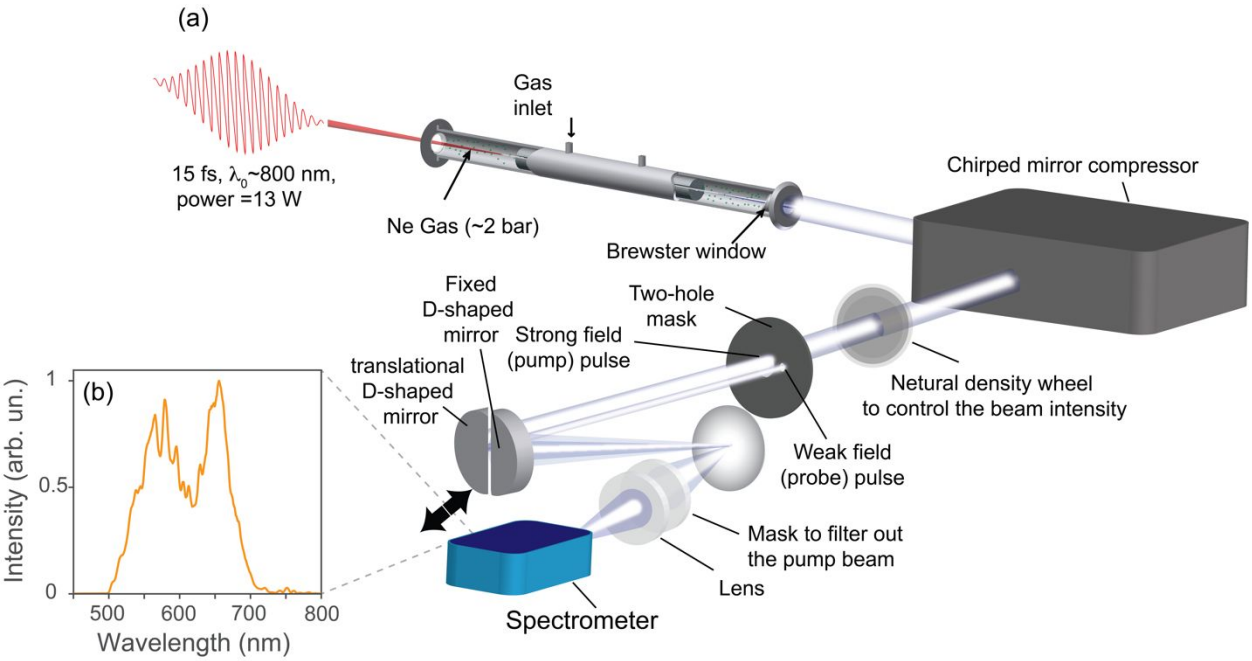

Fig. 1: (a) Attosecond All-optical Reflectivity Modulation (Atto-ARM) experiment setup to measure the reflectivity change in dielectric systems. The multi-cycle pulses spectrum is broadened by nonlinear propagation in Hollow-Core-Fiber (HCF). The broad-spectrum is compressed inside a chirped mirror compressor to 6.5 fs pulses. The output beam from the compressor is divided into the intense beam (pump) and the low power beam (probe) by a two-hole mask. A neutral density wheel filter is implemented in the beam path to control the input beam intensity. Two D-shape mirrors focus the two pump and probe beams on the dielectric sample. One of the D-shape mirrors is attached to a delay stage which moves with a nanometer resolution. The reflected pump beam is filtered out, and only the probe beam spectrum is focused and measured by an optical spectrometer. (b) The normalized measured probe spectrum, which is identical to the pump beam spectrum (spanning from 500 to 700 nm).

The pump beam triggers the transient phase transition and the reflectivity of the SiO_2 system. The reflectivity modulation can be traced by recording the spectrum of the reflected probe beam after filtering out the pump beam. Hence, the reflected probe beam is focused into an optical spectrometer. The spectrum is recorded as a function of the time delay between the pump and probe pulses, which is controlled by the delay stage with a step size of 100 as. The intensity of the reflected spectrum at each instance of time is integrated to obtain the TRM trace. The TRM represents the transient phase transition of the material in real-time. Then, to study the electronic delay response in SiO_2, the TRMs are recorded at different pump beam intensity levels ranging from ~$0.376x10^{13}$ to $1.315x10^{13}$ W/cm^2. At higher intensity, damage on the sample is observed, and the intensity modulation signal disappears. Note, the intensity level is controlled by rotating the metallic filter in the input beam path, so the ratio between the pump and probe beams remains the same at all measurements. Also, no change of the spectral phase and the CEP of the input beam pulse occurred during the measurements at different input beam intensities. In the second experiment, we replaced the SiO_2 sample with a 200 μm CaF_2 sample and acquired the TRM of CaF_2 at different pump beam intensities starting from ~$0.376x10^{13}$ to $1x10^{13}$ W/cm^2; the sample is damaged at higher intensity. These measurements enabled the study of the relative electronic delay response of CaF_2 and to compare these results with the electronic delay response of SiO_2 system.

Results and discussion

The transient photoinduced phase transition of fused silica in a strong field led to a change in the material properties and its reflectivity following the waveform of the pump field in real-time. Accordingly, the measurement of the TRM trace of fused silica provides access to the transient phase transient dynamics of SiO_2 in the strong field, which occurs in the sub-femtosecond time scale. Moreover, the TRM represents the vector potential of the driver field. Previously, we exploited this transient phase transition dynamics in SiO_2 to demonstrate the all-optical field sampling methodology[19]. Although, an important open question remains: is the induced transient phase transition dynamics of the dielectric system in strong field material-dependent? To answer this question, we measured the TRM of SiO_2 and CaF_2 and plotted in Fig. 2a & b, respectively. The retrieved electric field, by calculating the derivative of TRM of SiO_2 (Fig. 2a), is shown in a solid red line in Fig. 2c. The dashed blue line in Fig. 2c represents the electric field calculated from the derivative of the measured CaF_2 TRM (Fig. 2b). Remarkably, these results show that the transient phase transition dynamics is field-driven and independent of the dielectric system.

Correspondingly, the temporal profile of the pulse, retrieved from TRM in Fig. 2a & b, is shown in the dashed red and dashed blue lines, respectively, in Fig. 2d. In contrast, the measured temporal profile of the pump pulse by the conventional Transient Grating Frequency-Resolved Optical Gating (TG-FROG) is depicted in the solid black line in Fig. 2d. The temporal profiles from the measured TRMs of SiO_2 and CaF_2 are in excellent agreement with the measured profile by the TG-

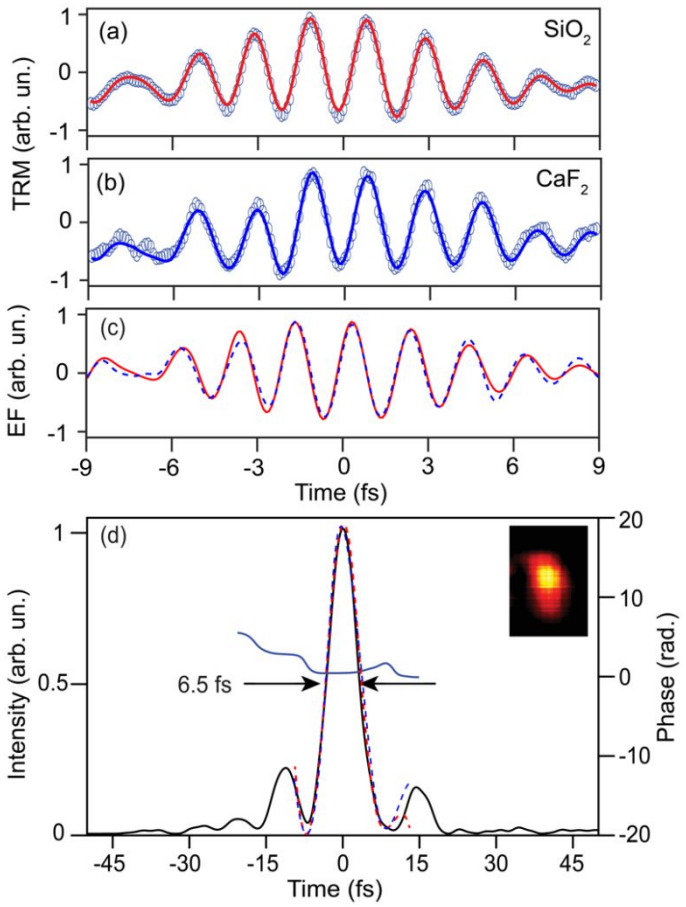

Fig. 2: (a) The measured total reflectivity modulation (TRM) trace of SiO_2. This trace is obtained by measuring the spectrum of the reflected probe beam from the front surface of SiO_2 as a function of the time delay between the pump and probe beams. Each point in the trace represents the integration of the probe spectrum at the corresponding time delay. (b) The measured TRM trace of CaF_2. (c) The electric fields calculated from the TRM trace in (a & b) are shown in solid red and dashed blue lines, respectively. The two calculated electric fields show a significant agreement indicating that the transient phase transition depends solely on the driver field. (d) The solid black line shows the temporal profile of the driver field pulse measured by TG-FROG. The Full-Width-Half Maximum (FWHM) pulse duration is 6.5 fs. The FROG trace is shown in the inset. The measured spectral phase is shown in the solid blue line. The temporal profiles calculated from the retrieved electric fields shown in (c) are depicted in the dashed red (from TRM of SiO_2) and the dashed blue line (from TRM of CaF_2).

FROG, confirming the all-optical field sampling methodology, based on the transient phase transition in SiO_2 ,and shows that this methodology is universal[19].

Nevertheless, the TRM measurements not only allowed to study the phase transition dynamics but also gave access to the related electron dynamics in the dielectric system. In the strong light field, the carriers are excited to the conduction band. After excitation, the field-driven intraband transition of the electrons in the conduction band occurs and causes the change in the optical properties and the reflectivity of the dielectric system. Therefore, the measurements of TRM traces at different driver field intensities provide insights into the electronic delay response of the dielectric system to the external light field.

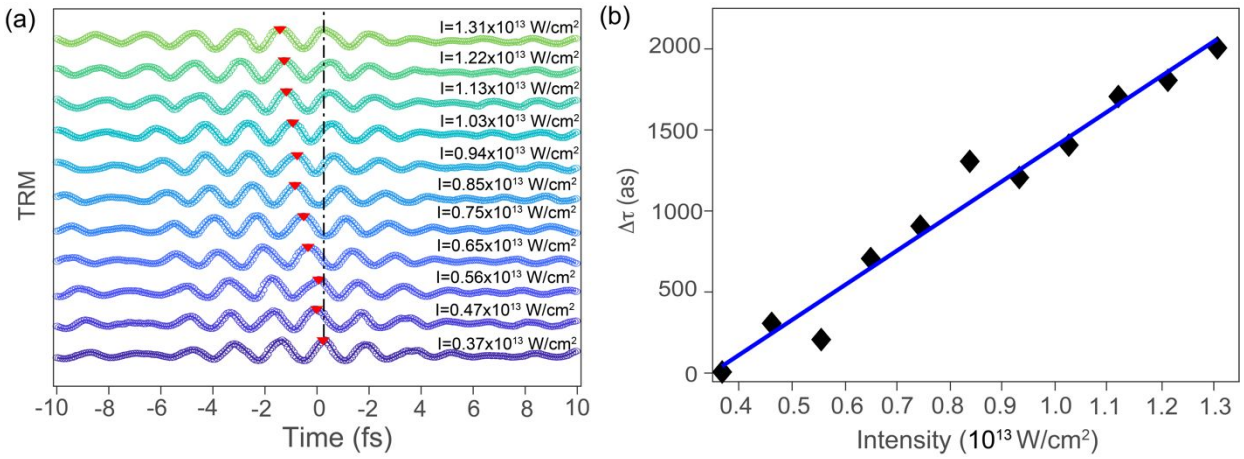

Fig. 3: (a) The measured TRM traces of SiO_2 at 11 different driver field intensities, ranging from 0.376x10^{13} to 1.31x10^{13} W/cm^2. The traces show a phase delay which increases at higher pump field intensity. The maxima of the highest (same) peaks of the measured TRM traces at different intensities are indicated with red arrows. The relative phase delay ($\Delta\tau$) between the TRM traces measured at each intensity is calculated by determining the delay between the maximum of the highest peak at this certain intensity and the maximum of the same peak at I=0.376x10^{13} W/cm^2. The black dashed line is a guide for the eye to show the relative delay increase. (b) The measured relative delay ($\Delta\tau$) as a function of the pump field intensity is shown in black points. The relative delay increases linearly as the pump intensity increases. The solid blue line shows the linear fitting of the measured relative delay.

Accordingly, we measured the TRM traces of SiO_2 under the exact same conditions at different field intensities ranging from ~0.376 to 1.315x10^{13} W/cm^2. The measured traces are normalized and plotted in Fig. 3a. As the intensity increase, the measured 11 TRM traces show a phase shift in the order of a few hundred attoseconds. The relative phase delay ($\Delta\tau$) is determined as the delay between the highest reflectivity peaks (marked by the red arrow in Fig. 3a) at a certain intensity

and the maximum of the corresponding peak at the lowest intensity (I ~0.376x10^{13} W/cm^2). The retrieved phase delay is plotted as a function of the driver field intensity in Fig. 3b. These measurements indicate that the electronic delay response increases linearly as the pump field intensity increases[27]. Moreover, from the slope of the linear relation in Fig. 3b, we can estimate the delay response at the ~0.376 x10^{13} W/cm^2 intensity to be roughly in the order of <800 attoseconds, under the assumption that linear relation is maintained at lower field intensities. The increase of the delay response at a higher pump field may be attributed to the increase in the excitation carrier density, AC Stark effect[29], and the system's polarizability[16, 17, 27].

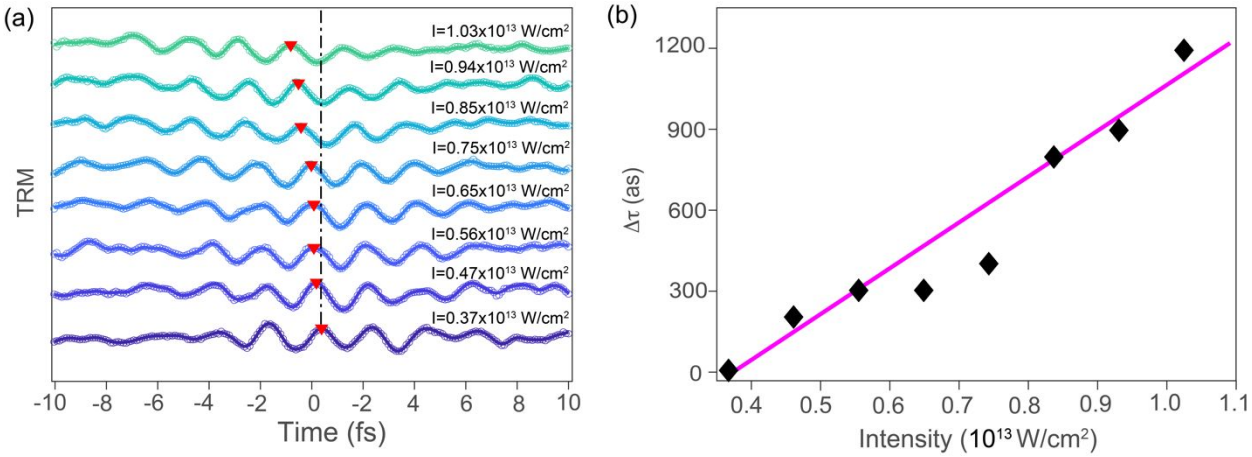

Fig. 4: (a) The measured TRM traces of CaF_2 at 8 different driver field intensities ranging from 0.376x10^{13} to 1.03x10^{13} W/cm^2. The traces show a phase delay which increases at higher pump field intensity. (b) The determined relative delay ($\Delta\tau$), between the maximum peak measured at the certain intensity with respect to the same peak at I=0.376x10^{13} W/cm^2, as a function of the pump field intensity is presented by black points. The relative delay increases linearly as the pump intensity increases similar to SiO_2. The solid magenta line shows the linear fitting of the measured relative delay.

Furthermore, we measured 8 TRM traces of CaF_2 at different pump field intensities (the results are shown in Fig. 4a). Also, the CaF_2 shows a phase retardation increase as the field intensity increases with a linear behavior, as shown in Fig. 4b. From the slope, we can estimate the delay response at I~0.376 x10^{13} W/cm^2 intensity to be in the order of ~650 attoseconds (assuming the delay response increase remains linear at lower intensity values), which is lower than the electronic delay response (~ 800 attoseconds) at the same intensity of SiO_2. This may be attributed to the difference in the bandgap value (~12 eV for CaF_2 and ~9 eV for SiO_2), the electronic structure, and the difference between the excited carrier density of both systems at the same field intensity

(I ~0.376 x10^{13} W/cm^2), which is theoretically calculated to be 6.58x10^{-10} nm^{-3} for CaF_2 and 7.3x10^{-7} nm^{-3} for SiO_2.

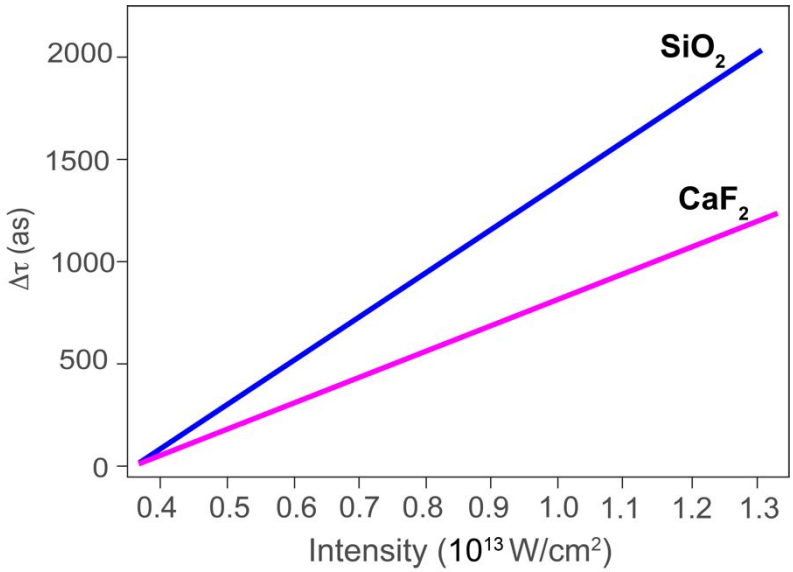

Fig. 5: The comparison between the linear behavior of the relative electronic delay response as a function of the pump field intensity measured for SiO_2 (in solid blue line) and CaF_2 (in solid magenta line) intensity increases. The two linear lines show different slops, indicating that the rise in the electronic delay response in SiO_2 at higher intensity is more than the increase in the electronic delay response in CaF_2.

To compare the behavior of the electronic delay repose of SiO_2 and CaF_2, we plot the fitted lines in Fig. 3b and Fig. 4b together in the same plot in Fig. 5. These results show that the electronic delay response of SiO_2 increases more at the same field intensity than in CaF_2. Accordingly, we can conclude that the electronic delay response behavior depends on the external field intensity, not on the type of the dielectric system (both systems show linear trending). Although, the electronic delay response value and the increasing increment as the driver field increases depend on the dielectric's bandgap and electronic structure.

Conclusions

We studied the transient phase transition dynamics of the SiO_2 and CaF_2 dielectric systems by tracing the optical reflectivity of the two systems in a strong field. The reported results confirm that the phase transition dynamics depend solely on the shape of the driver field waveform and not the type of the material. Moreover, we determined the relative electronic delay response on the two dielectric systems in different pump field intensities. The results show that the electronic delay response in the two dielectric

systems is linearly increased by increasing the driver field intensity. Although, the value of the electronic delay response and its increasing at a higher intensity pump field depends on the dielectric system and its electronic structure.

Author contributions

H.A., D.H., and M.S. conducted the experiments and analyzed the data. M.H. conceived, supervised, and directed the study. All authors discussed the results and their interpretation and wrote the manuscript.

Conflicts of interest

There are no conflicts of interest to declare.

Acknowledgments

This project is funded by the Air Force Office of Scientific Research under award number FA9550-19-1-0025 and partially funded by the Gordon and Betty Moore Foundation Grant GBMF7938. We are grateful for the W.M. Keck Foundation support. We thank Enam Chowdhury and Simin Zhang for the constructive discussion.

References

1. A. H. Zewail, *The Journal of Physical Chemistry A*, 2000, **104**, 5660-5694.
2. A. H. Zewail, *Angewandte Chemie International Edition*, 2000, **39**, 2586-2631.
3. M. Nisoli and G. Sansone, *Progress in Quantum Electronics*, 2009, **33**, 17-59.
4. F. Calegari, D. Ayuso, A. Trabattoni, L. Belshaw, S. De Camillis, S. Anumula, F. Frassetto, L. Poletto, A. Palacios, P. Decleva, J. B. Greenwood, F. Martín and M. Nisoli, *Science*, 2014, **346**, 336-339.
5. F. Calegari, G. Sansone, S. Stagira, C. Vozzi and M. Nisoli, *Journal of Physics B: Atomic, Molecular and Optical Physics*, 2016, **49**, 062001.
6. A. Schiffrin, T. Paasch-Colberg, N. Karpowicz, V. Apalkov, D. Gerster, S. Mühlbrandt, M. Korbman, J. Reichert, M. Schultze and S. Holzner, *Nature*, 2013, **493**, 70-74.
7. M. Schultze, E. M. Bothschafter, A. Sommer, S. Holzner, W. Schweinberger, M. Fiess, M. Hofstetter, R. Kienberger, V. Apalkov and V. S. Yakovlev, *Nature*, 2013, **493**, 75-78.
8. T. Paasch-Colberg, S. Y. Kruchinin, Ö. Sağlam, S. Kapser, S. Cabrini, S. Muehlbrandt, J. Reichert, J. V. Barth, R. Ernstorfer and R. Kienberger, *Optica*, 2016, **3**, 1358-1361.
9. T. T. Luu, M. Garg, S. Y. Kruchinin, A. Moulet, M. T. Hassan and E. Goulielmakis, *Nature*, 2015, **521**, 498-502.
10. F. Krausz and M. Ivanov, *Rev. Mod. Phys.*, 2009, **81**, 163.
11. F. Krausz, *Electrons in Motion: Attosecond Physics Explores Fastest Dynamics*, World Scientific Publishing Company Pte. Limited, 2019.
12. P. Corkum and F. Krausz, *Nature Physics*, 2007, **3**, 381-387.
13. G. Sansone, F. Kelkensberg, J. Pérez-Torres, F. Morales, M. F. Kling, W. Siu, O. Ghafur, P. Johnsson, M. Swoboda and E. Benedetti, *Nature*, 2010, **465**, 763-766.

14. V. S. Yakovlev, S. Y. Kruchinin, T. Paasch-Colberg, M. I. Stockman and F. Krausz, in *Ultrafast Dynamics Driven by Intense Light Pulses: From Atoms to Solids, from Lasers to Intense X-rays*, eds. M. Kitzler and S. Gräfe, Springer International Publishing, Cham, 2016, DOI: 10.1007/978-3-319-20173-3_12, pp. 295-315.
15. V. S. Yakovlev, M. I. Stockman, F. Krausz and P. Baum, *Scientific Reports*, 2015, **5**.
16. M. T. Hassan, T. T. Luu, A. Moulet, O. Raskazovskaya, P. Zhokhov, M. Garg, N. Karpowicz, A. M. Zheltikov, V. Pervak, F. Krausz and E. Goulielmakis, *Nature*, 2016, **530**, 66-70.
17. A. Wirth, M. T. Hassan, I. Grguraš, J. Gagnon, A. Moulet, T. T. Luu, S. Pabst, R. Santra, Z. A. Alahmed, A. M. Azzeer, V. S. Yakovlev, V. Pervak, F. Krausz and E. Goulielmakis, *Science*, 2011, **334**, 195-200.
18. M. T. Hassan, A. Wirth, I. Grguras, A. Moulet, T. T. Luu, J. Gagnon, V. Pervak and E. Goulielmakis, *Review of Scientific Instruments*, 2012, **83**, 111301.
19. D. Hui, H. Alqattan, S. Yamada, V. Pervak, K. Yabana and M. T. Hassan, *Nature Photonics*, 2022, **16**, 33-37.
20. G. Wachter, C. Lemell, J. Burgdörfer, S. A. Sato, X.-M. Tong and K. Yabana, *Physical review letters*, 2014, **113**, 087401.
21. J. B. Khurgin, *JOSA B*, 2016, **33**, C1-C9.
22. S. Yamada, M. Noda, K. Nobusada and K. Yabana, *Physical Review B*, 2018, **98**, 245147.
23. V. Apalkov and M. I. Stockman, *Physical Review B*, 2012, **86**, 165118.
24. K. Yabana, T. Sugiyama, Y. Shinohara, T. Otobe and G. Bertsch, *Physical Review B*, 2012, **85**, 045134.
25. T. Paasch-Colberg, S. Y. Kruchinin, Ö. Sağlam, S. Kapser, S. Cabrini, S. Muehlbrandt, J. Reichert, J. V. Barth, R. Ernstorfer, R. Kienberger, V. S. Yakovlev, N. Karpowicz and A. Schiffrin, *Optica*, 2016, **3**, 1358-1361.
26. S. Sato, K. Yabana, Y. Shinohara, T. Otobe and G. F. Bertsch, *Physical Review B*, 2014, **89**, 064304.
27. S. Sederberg, D. Zimin, S. Keiber, F. Siegrist, M. S. Wismer, V. S. Yakovlev, I. Floss, C. Lemell, J. Burgdörfer and M. Schultze, *Nature communications*, 2020, **11**, 1-8.
28. A. Korobenko, K. Johnston, M. Kubullek, L. Arissian, Z. Dube, T. Wang, M. Kübel, A. Y. Naumov, D. M. Villeneuve, M. F. Kling, P. B. Corkum, A. Staudte and B. Bergues, *Optica*, 2020, **7**, 1372-1376.
29. S. H. Autler and C. H. Townes, *Physical Review*, 1955, **100**, 703-722.